arXiv:1305.0055v2 [astro-ph.CO] 2 May 2013

Constraints on the Brans-Dicke gravity theory with the *Planck* data

Yi-Chao Li[1,2,*] Feng-Quan Wu[1,†] and Xuelei Chen[1,3‡]
[1] *National Astronomical Observatories, Chinese Academy of Sciences,*
20A Datun Road, Chaoyang District, Beijing 100012, China
[2] *University of Chinese Academy of Sciences, Beijing 100049, China*
[3] *Center of High Energy Physics, Peking University, Beijing 100871, China*

(Dated: May 3, 2013)

Based on the new cosmic microwave background (CMB) temperature data from the *Planck* satellite, the 9 year polarization data from the Wilkinson Microwave Anisotropy Probe (WMAP), and the baryon acoustic oscillation (BAO) distance ratio data from the Sloan Digital Sky Survey (SDSS) and 6 Degree field (6dF) surveys, we place a new constraint on the Brans-Dicke theory. We adopt a parametrization $\zeta = \ln(1 + \frac{1}{\omega})$, where the general relativity (GR) limit corresponds to $\zeta = 0$. We find no evidence of deviation from general relativity. At 95% probability, $-0.00246 < \zeta < 0.00567$, correspondingly, the region $-407.0 < \omega < 175.87$ is excluded. If we restrict ourselves to the $\zeta > 0$ (i.e. $\omega > 0$) case, then the 95% probability interval is $\zeta < 0.00549$, corresponding to $\omega > 181.65$. We can also translate this result to a constraint on the variation of gravitational constant, and find the variation rate today as $\dot{G} = -1.42^{+2.48}_{-2.27} \times 10^{-13}\mathrm{yr}^{-1}$ (1σ error bar), the integrated change since the epoch of recombination is $\delta G/G = 0.0104^{+0.0186}_{-0.0067}$ (1σ error bar). These limits on the variation of gravitational constant are comparable with the precision of solar system experiments.

I. INTRODUCTION

The Jordan-Fierz-Brans-Dicke theory [1–5] (hereafter the Brans-Dicke theory for simplicity) is the simplest extended theory of gravity. In addition to the metric tensor, there is a scalar field ϕ in this theory, i.e. the Brans-Dicke field, which gives the effective gravitational constant[6–10]. The action in the Jordan frame is

$$\mathcal{S} = \frac{1}{16\pi}\int d^4x\sqrt{-g}\left[-\phi R + \frac{w}{\phi}g^{\mu\nu}\nabla_\mu\phi\nabla_\nu\phi\right] + \mathcal{S}^{(m)} \ , \tag{1}$$

where $\mathcal{S}^{(m)}$ is the action for the matter field. Here ϕ is the Brans-Dicke field and ω is the Brans-Dicke parameter. In the limit of $\omega \to \infty$ the Brans-Dicke theory is reduced to Einstein's general relativity theory.

Solar system experiments have already put very stringent constraints on the Brans-Dicke model[11, 12]. For example, the tracking data obtained from the Cassini mission gives $\omega > 40000$ at the 2σ level [13]. Nevertheless, it is still interesting to test the theory on cosmological scales, especially because the Brans-Dicke theory may be regarded as an approximation for a number of scalar-tensor theories of gravity which have more significant effects on larger scales. The cosmic microwave background (CMB) anisotropy can be calculated for a given theory, and the Brans-Dicke model may be tested with high precision [14].

A number of limits on the ω parameter have been derived since WMAP released its data on CMB anisotropy. Acquaviva et al. report that $\omega > 80$ at 99% level by combining the WMAP 1st year data and some ground or balloon based experiments and the large scale structure data[15]. Wu et al. [16, 17] excluded the region of $-120 < \omega < 97.8$ by using the WMAP 5 year data and the Sloan Digital Sky Survey (SDSS) Luminous Red Galaxy (LRG) data. Considering only the possibility of $\omega > 0$, Avilez and Skordis[18] derived a limit of $\omega > 288$ at 95% confidence level. by combining the WMAP 7 year data and the data from the South Pole Telescope (SPT) and other small scale CMB experiments. When comparing these different results, one should note that the limits obtained depend very much on the parameterization and prior used, see the next section for discussion.

The precision of cosmological observations are being improved steadily. The WMAP group have published the data of 9 years of observation [19, 20], and recently, the Planck collaboration published their observational results [21]. In addition to the CMB observations, there are also much progress in redshift surveys of galaxies. Recent surveys such as the SDSS-III Baryon Oscillation Spectroscopic Survey (BOSS) [1] and 6dF [2] have measured the power spectrum of the large scale structure at different redshifts, and obtained cosmic distances from the baryon acoustic oscillation features.

In this paper, we update the constraint on the Brans-Dicke model by using the new CMB data [3], including the Planck temperature anisotropy [22] and the the WMAP9 CMB polarization data[19]. Following the Planck collaboration [23], in addition to the CMB data, we also use the BAO data from the SDSS [24–26] and 6dF [27] galaxy redshift surveys.

---

[*] Electronic address: ycli@bao.ac.cn
[†] Electronic address: wufq@bao.ac.cn
[‡] Electronic address: xuelei@cosmology.bao.ac.cn

[1] http://www.sdss3.org/surveys/boss.php

[2] http://www.aao.gov.au/6dFGS/

[3] http://lambda.gsfc.nasa.gov/

II. METHODS

For convenience, we introduce a dimensionless field $\varphi = G\phi$ where G is the Newtonian gravitational constant, then the Einstein equations are

$$G_{\mu\nu} = \frac{8\pi G}{\varphi}T^{(m)}_{\mu\nu} + \frac{\omega}{\varphi^2}(\nabla_\mu\varphi\nabla_\nu\varphi - \frac{1}{2}g_{\mu\nu}\nabla_\lambda\varphi\nabla^\lambda\varphi) + \frac{1}{\varphi}(\nabla_\mu\nabla_\nu\varphi - g_{\mu\nu}\nabla_\lambda\nabla^\lambda\varphi) \ , \quad (2)$$

where $T^{(m)}_{\mu\nu}$ is the stress tensor for matter. The equation of motion for φ is

$$\nabla_a\nabla^a\varphi = \frac{\kappa}{2\omega+3}T^{(m)\mu}_{\nu} \ . \quad (3)$$

For G to be consistent with the Cavendish experiment, The value of φ at present day should be

$$\varphi_0 = \frac{2\omega+4}{2\omega+3} \ . \quad (4)$$

We follow the calculation method described in [16], in which we developed the covariant and gauge-invariant formalism of cosmological perturbation theory in the case of Brans-Dicke gravity, and apply the method to calculate the angular power spectra of CMB temperature and polarizations, as well as the power spectrum of large scale structure (LSS).

Given a cosmological model, the angular power spectra of CMB temperature and polarization and the matter power spectrum can be calculated, for example with the publicly available code `CAMB` [28]. In order to constrain the cosmological parameters with the observational data, we use the publicly available CosmoMC code [29], which uses the Markov Chain Monte Carlo (MCMC) method to explore the parameter space, with a modified `CAMB` code developed by Wu et al. in Ref [17]. We use the latest CMB data published by the Planck team [22]. According to our previous analysis [16], the small scale (high-l) anisotropy is affected more by the Brans-Dicke gravity, so the more precise measurements of *Planck* on small scales (up to $l \sim 2500$) should help greatly. For the low-ls, we also include the TE and BB power spectrum estimated from the polarization map of WMAP9, though the latter does not provide much distinguishing power at present.

We also combine the BAO data from large scale structure surveys, including the SDSS DR7 [24, 25], BOSS DR9 [26] and 6dF [27]. The BAO surveys measure the distance ratio

$$d_z = \frac{r_s(z_{drag})}{D_V(z)} \ , \quad (5)$$

where $r_s(z_{drag})$ is the comoving sound horizon when baryons became dynamically decoupled from photons (the baryon drag epoch) and $D_V(z)$ is the combination of angular-diameter distance, $D_A(z)$, and the Hubble parameter, $H(z)$

$$D_V(z) = [(1+z)^2 D_A^2(z)\frac{cz}{H(z)}]^{1/3} \ . \quad (6)$$

We follow the choice of BAO data set "SDSS DR7 + BOSS DR9 + 6dF" in the Planck analysis [22]. This includes two of the most accurate BAO measurements, and minimizes the correlations between the galaxy surveys, as the two surveys have widely separated effective redshifts.

The derived limits depend on which parameterization is selected and how the priors are set. As the experiments so far all favors the GR case and the Brans-Dicke parameter is stringently constrained, it is more convenient to take the GR as the null case, and have a parametrization in which the tested parameter vanishes for GR. In practice a flat prior on a finite range is usually assigned to the parameter. For example, Ref.[15] and Ref.[18] considered flat prior on $\ln[1/\omega]$ (though the exact parameter they used differs slightly). A limitation of this choice is that it could not treat the $\omega < 0$ case. Ref.[18] argued that if $\omega < -3/2$ the Brans-Dicke field would be a ghost field, and they will therefore consider only positive ω. However, we would rather err on the conservative side, and use a more general form of parameterization which allows negative ω. Indeed, at present there are many phantom dark energy [30] models in which the field are also ghost-like. In Ref.[17] we used

$$\zeta = \ln(1+\frac{1}{\omega}) \ , \quad (7)$$

in the present paper we will also adopt this parameterization. This parameter has the nice property that as $\zeta \to 0$, the Brans-Dicke theory reduces to Einstein gravity, and it is easy to obtain limits on both the negative and positive value of ω. We choose the same initial range $[-0.014, 0.039]$ as Wu et al. in [17], which is convenient for computation, while at the same time the final constraint is not very sensitive to this range, since at the edge of the prior range the likelihood is very small. In fact, if one wishes to consider only positive values of ω, we can also do that by simply restricting the range of the prior to $0 < \zeta < 0.039$.

As pointed out by Ref.[18], comparing with their prior, our flat prior on ζ penalizes large ω, and hence for the same data set a "weaker" limit on ω would be obtained for our choice. We do not see a good theoretical reason to favor one prior on ω over the other, but our choice is again in agreement with our general philosophy of being conservative on constraining models. We remind the reader to notice the effect of the prior when comparing results obtained in different papers.

We also obtain limits on the following basic or derived cosmological parameters: Ω_Λ, $\Omega_{\rm b}h^2$, $\Omega_{\rm c}h^2$, θ, τ, $n_{\rm s}$, $\ln(10^{10}A_{\rm s})$, Age/Gyr, σ_8, $z_{\rm re}$ and H_0. Here Ω_Λ is the dark energy density today. $\Omega_{\rm b}$ is the baryon density today. $\Omega_{\rm c}$ is the cold dark matter density today. θ is the angular scalar of the sound horizon at last-scattering. τ is the Thomson scattering optical depth due to the reionization. $n_{\rm s}$ is the scalar spectrum power-law index. $\ln(10^{10}A_{\rm s})$ is log power of the primordial curvature perturbations. Age/Gyr is the age of the universe. σ_8 is the rms matter fluctuations today in linear theory. $z_{\rm re}$ is the redshift at which universe is half reionized. H_0 is the Hubble constant.

III. RESULTS

Fig.1 shows the 1-D marginalized distribution for the Brans-Dicke parameter ζ. The curve which is labelled as "Planck + WP" shows the CMB-only result, for which the temperature data from Planck and the polarization data from WMAP9 is used. The curve which is labelled as "Planck + WP + BAO" combined the CMB data with the BAO observation data from SDSS DR7, BOSS DR9 and 6dF. For comparison, we also plot in this figure the result obtained in our previous work [17], which used the WMAP5 data and the matter power spectrum from the SDSS LRG survey.

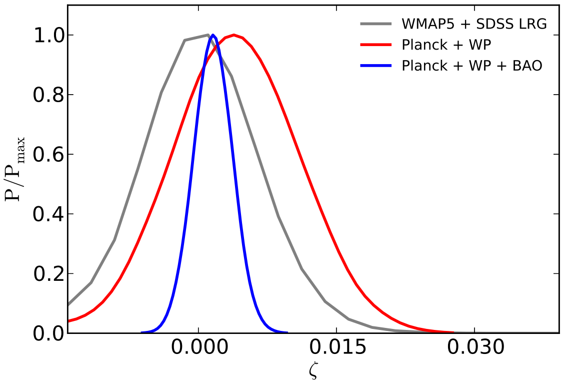

FIG. 1: The one dimensional likelihood distribution for ζ. "Planck + WP" denotes the result of using Planck temperature data as well as WMAP9 polarization data. "Planck + WP + BAO" denotes the combined constraint with BAO data [24] [25] [26] [27]. We also plot the result in previous work [17], "WMAP5 + SDSS LRG", which is using CMB temperature and polarization data from WMAP5, combined with matter power spectrum measured with the luminous red galaxy (LRG) survey of the SDSS.

Comparing with the previous work, especially Wu et al.[17], which used the same parameterization, the constraints become stronger, and the new data favors a slightly more positive value of ζ. The likelihood of the CMB-only data looks quite Gaussian. Because of the high angular resolution of Planck data, the CMB-only data can already give better constraints than before. With the BAO data, the constraint is further tightened. The BAO distances estimated from galaxy surveys play the same role as the matter power spectrum in distinguishing the different models.

For the CMB-only case, we find the 68% and 95% intervals are

$$-0.247\times10^{-2} < \zeta < 1.080\times10^{-2} \quad (68\%)\ ; \qquad (8)$$
$$-0.855\times10^{-2} < \zeta < 1.716\times10^{-2} \quad (95\%)\ . \qquad (9)$$

These correspond to

$$\omega < -405.36 \quad \text{or} \quad \omega > 92.09 \quad (68\%)\ ; \qquad (10)$$
$$\omega < -117.46 \quad \text{or} \quad \omega > 57.78 \quad (95\%)\ . \qquad (11)$$

We see that with the CMB data alone, the constraint is still relatively loose.

Addition of the BAO data helps to break the parameter degeneracy, and much stronger limits are obtained. For the CMB+BAO case, we find the 68% and 95% bounds are

$$-0.046\times10^{-2} < \zeta < 0.366\times10^{-2} \quad (68\%)\ ; \qquad (12)$$
$$-0.246\times10^{-2} < \zeta < 0.567\times10^{-2} \quad (95\%)\ , \qquad (13)$$

which correspond to

$$\omega < -2174.41 \quad \text{or} \quad \omega > 272.72 \quad (68\%)\ ; \qquad (14)$$
$$\omega < -407.00 \quad \text{or} \quad \omega > 175.87 \quad (95\%)\ . \qquad (15)$$

If we restrict ourselves to the case of $\zeta > 0$, or equivalently $\omega > 0$, then for the CMB only case the 68% and 95% bounds are

$$0 < \zeta < 0.895\times10^{-2} \quad (68\%)\ ; \qquad (16)$$
$$0 < \zeta < 1.645\times10^{-2} \quad (95\%)\ , \qquad (17)$$

corresponding to

$$\omega > 111.23 \quad (68\%); \qquad \omega > 60.29 \quad (95\%)\ . \qquad (18)$$

For the CMB+BAO case,

$$0 < \zeta < 0.296\times10^{-2} \quad (68\%)\ ; \qquad (19)$$
$$0 < \zeta < 0.549\times10^{-2} \quad (95\%)\ , \qquad (20)$$

corresponding to

$$\omega > 337.34 \quad (68\%); \qquad \omega > 181.65 \quad (95\%)\ . \qquad (21)$$

We see that the constraints are only slightly different from their respective positive bounds where $\zeta < 0 (\omega < 0)$ are allowed, even though the *a prior* allowed parameter space is smaller. This shows that the negative ζ solutions fit about also very well, so reduction of parameter space does not significantly improve the constraint.

As discussed in the last section, these limits depend on the parameterization and prior adopted. The results presented here applies to the parameter ζ, even though we also quoted limits on ω since that's what appeared in the Brans-Dicke theory. This parameterization is more "conservative", so our limits appeared to be "weaker" than Ref.[18] even though we have used the newer and more precise Planck data.

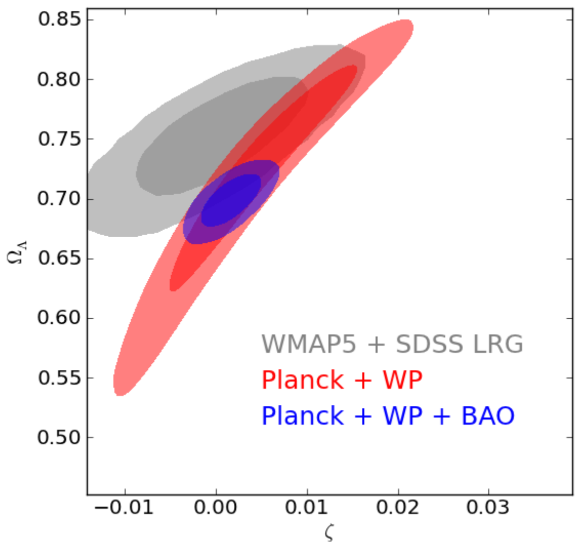

FIG. 2: The two dimensional contour for ζ against Ω_Λ.

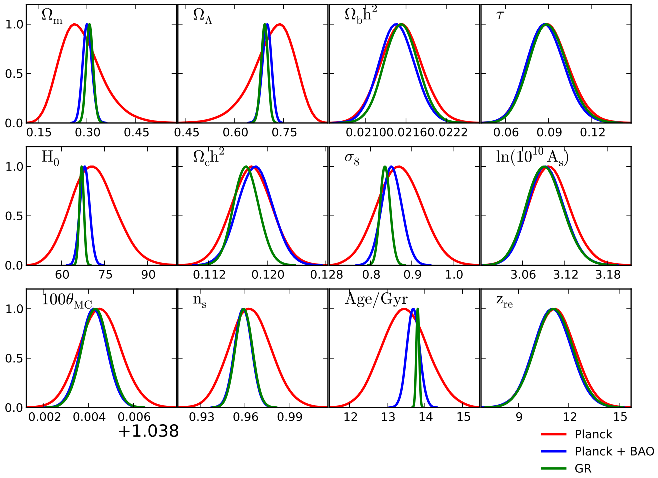

FIG. 3: The one dimensional likelihood for cosmological parameters. The red lines with label “Planck” represent the result with Planck temperature data and WMAP9 polarization data; the blue lines with label “Planck + BAO” denote the result combined with BAO data; the green line labelled “GR” is the result of fixing $\zeta = 0$, in which case the Brans-Dicke gravity reduces to Einstein theory.

Fig.2 shows the two dimensional contours for ζ against Ω_Λ. If only the CMB data from Planck is used, the constraint already become stronger, but there is significant degeneration between ζ and Ω_Λ. The BAO data can help to break the degeneration and give much stronger constraints. The center of the contours shifted somewhat from the center of our previous results, this is the same trend as seen in the fitting of the standard cosmological model, for Ω_Λ is lowered, but we see that the shift on the center of ζ is small.

Next we examine how the constraints on other cosmological parameters are affected if we consider the Brans-Dicke gravity. Fig.3 shows the one dimensional likelihood for some cosmological parameters. In this plot, we show the result with ζ fixed to 0, labelled as “GR”, in this case the Brans-Dicke theory is reduced to the standard ΛCDM model with Einstein's General Relativity. It is obvious from the figure that when the BAO data are combined, the constraint is much tighter than the case with CMB data only. However, for most parameters, the likelihood distribution of the GR case and the Brans-Dicke case is very similar, the shifts in the best fit parameters (peak value of the likelihood) are small, and the differences in the width of the likelihood are also relatively small, showing that the addition of the Brans-Dicke parameter does not significantly affect the uncertainty in other cosmological parameters. The most affected basic parameters are H_0, $\Omega_c h^2$, and σ_8, while for the derived parameters the uncertainty on the cosmic age is much larger.

We also plot the two dimensional contours in Fig.5. The Planck data can give accurate measure on $\Omega_b h^2$ without other additional data, thanks to the well measured peaks in angular power spectra. The degeneracy between ζ and $\Omega_b h^2$, as well as $\Omega_c h^2$ are quite limited and the uncertainty of fitting is reduced. The degeneracy between ζ and Ω_m, Ω_Λ are broken by BAO data, which could also be seen in one dimensional likelihood distribution, Ω_m and Ω_Λ change greatly after introducing BAO data.

The best-fit values and 68% marginalized error are shown in Table II. For comparison, in Table II we also list the results for Einstein gravity given in Ref.[22]. The Einstein result is constrained by using Planck low-l and high-l data, as well as WMAP9 polarization data and BAO data, which is the same as our data set. Comparing with the WMAP data, the Planck data favors lower Ω_Λ and lower H_0, in the standard ΛCDM model fitting. This trend was noted by the Planck team and also found in our model.

There are some slight differences between our results with ζ fixed to 0 and the result published by the Planck team [23]. The differences come mainly from different setting of parameters in CosmoMC. In our fitting, in order to focus on the Brans-Dicke parameters, we ignored the effect of massive neutrinos, and fixed the neutrino number. The best-fit values of cosmological parameters in our Brans-Dicke model are consistent with ΛCDM model in Einstein theory.

We can also test the variation of the gravitational constant G in the context of Brans-Dicke theory. We added two derived parameters in the MCMC code, i.e. $\dot{G}/G \equiv -\dot{\varphi}/\varphi$, which is the change rate of gravitational constant at present, and $\delta G/G \equiv (G_{rec} - G_0)/G_0$, which is the integrated change of gravitational constant since the epoch of recombination. The one dimensional marginalized likelihood is shown in Fig.4(a) and Fig.4(b). The likelihood functions are fairly close to the Gaussian form. We can take the 68% limit as corresponding to the 1σ error for these measurements.

For the CMB only case, the best-fit values are

$$\dot{G}/G = -0.4617 \times 10^{-12}, \qquad \delta G/G = 0.0318$$

and the 68% marginalized limits are

$$\begin{aligned} -1.1970 \times 10^{-12} < \ & \dot{G}/G \ < 0.4597 \times 10^{-12}; && (22) \\ -0.0197 < \ & \delta G/G \ < 0.0835 && (23) \end{aligned}$$

For the CMB+BAO case,

$$\dot{G}/G = -0.1417 \times 10^{-12}, \qquad \delta G/G = 0.0104$$

and the 68% marginalized limits are

$$\begin{aligned} -0.4082 \times 10^{-12} < \ & \dot{G}/G \ < 0.0663 \times 10^{-12} && (24) \\ -0.0037 < \ & \delta G/G \ < 0.0290 && (25) \end{aligned}$$

We list the constraints on $\dot{G}/G$ with different methods in Table I. Though model-dependent, our cosmological constraints are now comparable in precision with other methods, including the solar system experiments.

TABLE I: Constraints on the rate of variations of gravitational constant. The errors are 1σ unless otherwise noted.

$\dot{G}/G$ $[10^{-13}\mathrm{yr}^{-1}]$	Method
2 ± 7	lunar laser ranging [31]
0 ± 4	big bang nucleosynthesis [32][33]
0 ± 16	helioseismology [34]
-6 ± 20	neutron star mass [35]
20 ± 40	Viking lander ranging [36]
40 ± 50	binary pulsar [37]
$-96 \sim 81$ (2σ)	CMB (WMAP3) [38]
$-17.5 \sim 10.5$ (2σ)	WMAP5+SDSS LRG [17]
$-1.42^{+2.48}_{-2.27}$ (1σ)	Planck+WP+BAO (This paper)

IV. SUMMARY

In this paper, we use the newly published Planck CMB temperature data [22] and the WMAP 9 year CMB polarization data [19] to constrain the Brans-Dicke theory. In addition to the Planck data, we also use the BAO data from the SDSS DR7 [24] [25], BOSS DR9 [26] and 6dF[27], which help to break parameter degeneracy.

We use the parameterization $\zeta = \ln(1 + \frac{1}{\omega})$ introduced in Ref.[17], for which the GR limit is achieved when $\zeta \to 0$, $(|\omega| \to \infty)$. This parameterization may be more "conservative" than some of the other parameterizations, so the limit we derive may also appear "weaker" than given in some of the other works. The readers should note this when comparing the results given in different works.

We obtained constraints by using the CMB data (referred to as CMB-only). The 68% and 95% bounds are given Eqs.(8)-(11). By combining the BAO data, we obtain stricter constraints, which are given in Eqs.(12)-(15). We also considered the bounds obtained if $\zeta > 0$ (or equivalently $\omega > 0$) is assumed to be positive, these are given in Eqs.(16)-(21). We do not detect any significant deviation from Einstein's general theory of relativity, and the constraint on the Brans-Dicke model is tightened compared with previous results.

We examined the distribution of other cosmological parameters. For most parameters, the best fit values and measurement errors are not altered much by the introduction of the Brans-Dicke gravity. The most affected parameters are H_0, $\Omega_c h^2$, and σ_8, and the derived parameter of cosmic age.

Finally, the variation of the gravitational constant in the Brans-Dicke model are also constrained, the results are given in Eqs.(22)-(25), and also summarized in Table I. These constraints are model-dependent, nonetheless, it is remarkable that the limits obtained are comparable with the constraints from the highly precise solar system experiments.

Acknowledgements

We thank Antony Lewis and Xiaoyuan Huang for their helps on the CosmoMC code. Our MCMC computation was performed on the Laohu cluster in NAOC. This work is supported by the Ministry of Science and Technology 863 project grant 2012AA121701, the NSFC grant 11073024, 11103027, and the CAS Knowledge Innovation grant KJCX2-EW-W01.

---

[1] P. Jordan, Nature (London) **164**, 637 (1949).
[2] P. Jordan, Z. Phys. **157**, 112 (1959).
[3] M. Fierz, Helv. Phys. Acta **29**, 128 (1956).
[4] C. Brans and R. H. Dicke, Phys. Rev. **124**, 925 (1961).
[5] R. H. Dicke, Phys. Rev. **125**, 2163 (1962).
[6] P. G. Bergmann, Int. J. Theor. Phys. **1**, 25 (1968).
[7] J. Nordtvedt, Kenneth, Astrophys. J. **161**, 1059 (1970).
[8] R. V. Wagoner, Phys. Rev. **D1**, 3209 (1970).

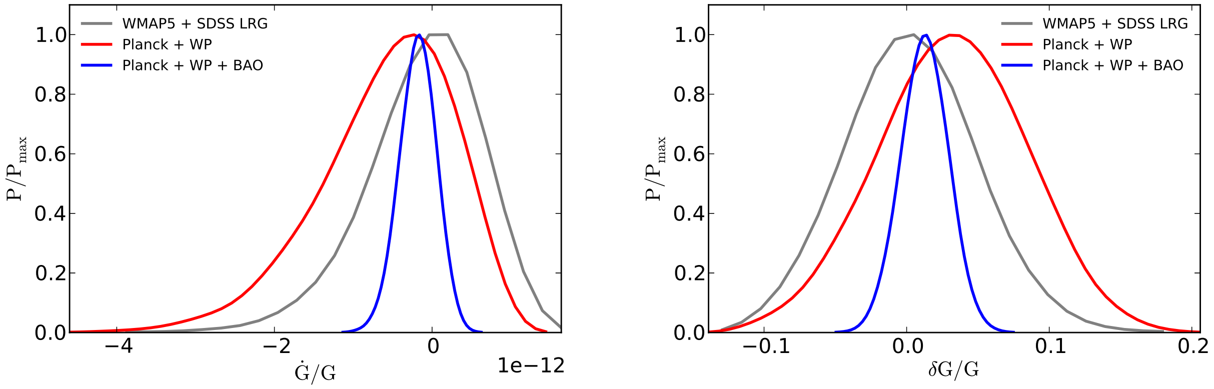

(a)

(b)

FIG. 4: Fig.4(a), and Fig.4(b) show the one dimensional marginalized likelihood of parameters $\dot{G}/G$ and $\delta G/G$.

[9] J. D. Bekenstein, Phys. Rev. **D15**, 1458 (1977).

[10] J. D. Bekenstein and A. Meisels, Phys. Rev. **D18**, 4378 (1978).

[11] C. M. Will, *Theory and experiment in gravitational physics* (1981).

[12] C. M. Will, Living Reviews in Relativity **9**, 3 (2006).

[13] B. Bertotti, L. Iess, and P. Tortora, Nature **425**, 374 (2003).

[14] X. Chen and M. Kamionkowski, Phys. Rev. **D60**, 104036 (1999), astro-ph/9905368.

[15] V. Acquaviva, C. Baccigalupi, S. M. Leach, A. R. Liddle, and F. Perrotta, Phys. Rev. **D71**, 104025 (2005), astro-ph/0412052.

[16] F.-Q. Wu, L.-E. Qiang, X. Wang, and X. Chen, Phys. Rev. D **82**, 083002 (2010), 0903.0384.

[17] F.-Q. Wu and X. Chen, Phys. Rev. D **82**, 083003 (2010), 0903.0385.

[18] A. Avilez and C. Skordis (2013).

[19] C. L. Bennett, D. Larson, J. L. Weiland, N. Jarosik, G. Hinshaw, N. Odegard, K. M. Smith, R. S. Hill, B. Gold, M. Halpern, et al., ArXiv e-prints (2012), 1212.5225.

[20] G. Hinshaw, D. Larson, E. Komatsu, D. N. Spergel, C. L. Bennett, J. Dunkley, M. R. Nolta, M. Halpern, R. S. Hill, N. Odegard, et al., ArXiv e-prints (2012), 1212.5226.

[21] Planck Collaboration, P. A. R. Ade, N. Aghanim, C. Armitage-Caplan, M. Arnaud, M. Ashdown, F. Atrio-Barandela, J. Aumont, C. Baccigalupi, A. J. Banday, et al., ArXiv e-prints (2013), 1303.5062.

[22] P. collaboration, P. A. R. Ade, N. Aghanim, C. Armitage-Caplan, M. Arnaud, M. Ashdown, F. Atrio-Barandela, J. Aumont, C. Baccigalupi, A. J. Banday, et al. (2013).

[23] Planck Collaboration, P. A. R. Ade, N. Aghanim, C. Armitage-Caplan, M. Arnaud, M. Ashdown, F. Atrio-Barandela, J. Aumont, C. Baccigalupi, A. J. Banday, et al., ArXiv e-prints (2013), 1303.5076.

[24] W. J. Percival, B. A. Reid, D. J. Eisenstein, N. A. Bahcall, T. Budavári, J. A. Frieman, M. Fukugita, J. E. Gunn, Ž. Ivezić, G. R. Knapp, et al., Monthly Notices of the Royal Astronomical Society **401**, 2148 (2010).

[25] N. Padmanabhan, X. Xu, D. J. Eisenstein, R. Scalzo, A. J. Cuesta, K. T. Mehta, and E. Kazin, Monthly Notices of the Royal Astronomical Society **427**, 2132 (2012).

[26] L. Anderson, E. Aubourg, S. Bailey, D. Bizyaev, M. Blanton, A. S. Bolton, J. Brinkmann, J. R. Brownstein, A. Burden, A. J. Cuesta, et al. (2012).

[27] F. Beutler, C. Blake, M. Colless, D. H. Jones, L. Staveley-Smith, L. Campbell, Q. Parker, W. Saunders, and F. Watson, Monthly Notices of the Royal Astronomical Society **416**, 3017 (2011).

[28] A. Lewis and A. Challinor, *http://camb.info/* (1999).

[29] A. Lewis and S. Bridle, Phys. Rev. **D66**, 103511 (2002), astro-ph/0205436.

[30] R. R. Caldwell, M. Kamionkowski, and N. N. Weinberg, Physical Review Letters **91**, 071301 (2003), arXiv:astro-ph/0302506.

[31] J. Muller and L. Biskupek, Class. Quant. Grav. **24**, 4533 (2007).

[32] C. J. Copi, A. N. Davis, and L. M. Krauss, Phys. Rev. Lett. **92**, 171301 (2004), astro-ph/0311334.

[33] C. Bambi, M. Giannotti, and F. L. Villante, Phys. Rev. **D71**, 123524 (2005), astro-ph/0503502.

[34] D. B. Guenther, L. M. Krauss, and P. Demarque, Astrophys. J. **498**, 871 (1998).

[35] S. E. Thorsett, Phys. Rev. Lett. **77**, 1432 (1996), astro-ph/9607003.

[36] R. W. Hellings, P. J. Adams, J. D. Anderson, M. S. Keesey, E. L. Lau, E. M. Standish, V. M. Canuto, and I. Goldman, Physical Review Letters **51**, 1609 (1983).

[37] V. M. Kaspi, J. H. Taylor, and M. F. Ryba, Astrophys. J. **428**, 713 (1994).

[38] K.-C. Chang and M. C. Chu, Phys. Rev. **D75**, 083521 (2007), astro-ph/0611851.

TABLE II: Summary of cosmological parameters and the corresponding 68% intervals. The “Planck + WP” column lists the result of using temperature map from Planck and polarization map from WMAP9; The “Planck + WP + BAO” column lists the result with BAO data combined; We also list the result using the same data as “Planck + WP + BAO”, but fix $\zeta = 0$ in the “Planck + WP + BAO with $\zeta = 0$” column, that Brans-Dicke reduces to Einstein theory. The last column is the result form Planck team in Ref.[22].

	Brans-Dicke						Einstein[22]	
	Planck + WP		Planck + WP + BAO		Planck + WP + BAO with $\zeta = 0$		Planck + WP + BAO	
Parameter	Best fit	68% limits	Best fit	68% limits	Best fit	68% limits	Best fit	68% limits
Ω_m	0.2821	$0.2845^{+0.0479}_{-0.0753}$	0.3048	$0.3016^{+0.0133}_{-0.0149}$	0.3098	$0.3087^{+0.0101}_{-0.0110}$		
Ω_Λ	0.7179	$0.7155^{+0.0753}_{-0.0479}$	0.6952	$0.6984^{+0.0149}_{-0.0133}$	0.6902	$0.6913^{+0.0110}_{-0.0101}$	0.6914	$0.692^{+0.01}_{-0.01}$
$\Omega_{\rm b} h^2$	0.0215	$0.0215^{+0.0003}_{-0.0003}$	0.0215	$0.0215^{+0.0003}_{-0.0003}$	0.0215	$0.0215^{+0.0002}_{-0.0002}$	0.0222	$0.0221^{+0.0002}_{-0.0002}$
τ	0.0802	$0.0902^{+0.0128}_{-0.0150}$	0.0871	$0.0883^{+0.0122}_{-0.0136}$	0.0830	$0.0899^{+0.0124}_{-0.0137}$	0.0952	$0.092^{+0.013}_{-0.013}$
H_0	70.4907	$71.2328^{+7.1229}_{-8.2356}$	67.7905	$68.1442^{+1.6147}_{-1.6225}$	66.9751	$67.0443^{+0.7621}_{-0.7665}$	67.77	$67.80^{+0.77}_{-0.77}$
$\Omega_{\rm c} h^2$	0.1187	$0.1179^{+0.0027}_{-0.0027}$	0.1186	$0.1184^{+0.0023}_{-0.0023}$	0.1174	$0.1172^{+0.0017}_{-0.0017}$	0.1189	$0.1187^{+0.0017}_{-0.0017}$
σ_8	0.8648	$0.8705^{+0.0526}_{-0.0524}$	0.8507	$0.8519^{+0.0239}_{-0.0238}$	0.8314	$0.8357^{+0.0115}_{-0.0125}$	0.8288	$0.826^{+0.012}_{-0.012}$
$\ln(10^{10} A_{\rm s})$	3.0810	$3.0989^{+0.0268}_{-0.0305}$	3.0922	$3.0937^{+0.0242}_{-0.0264}$	3.0797	$3.0921^{+0.0245}_{-0.0270}$	3.0973	$3.091^{+0.025}_{-0.025}$
$100\theta_{\rm MC}$	1.0423	$1.0425^{+0.0009}_{-0.0009}$	1.0424	$1.0422^{+0.0006}_{-0.0006}$	1.0424	$1.0423^{+0.0006}_{-0.0006}$	1.0415	$1.0415^{+0.0006}_{-0.0006}$
$n_{\rm s}$	0.9621	$0.9638^{+0.0138}_{-0.0137}$	0.9606	$0.9588^{+0.0056}_{-0.0056}$	0.9584	$0.9593^{+0.0056}_{-0.0056}$	0.9611	$0.9608^{0.0054}_{-0.0054}$
Age/Gyr	13.4843	$13.4730^{+0.5892}_{-0.5924}$	13.7179	$13.6921^{+0.1637}_{-0.1644}$	13.8100	$13.8119^{+0.0371}_{-0.0371}$	13.7965	$13.798^{+0.037}_{-0.037}$
$z_{\rm re}$	10.3531	$11.1855^{+1.1645}_{-1.1589}$	10.9543	$11.0309^{+1.0948}_{-1.0862}$	10.5331	$11.1067^{+1.0993}_{-1.0984}$	11.52	$11.3^{+1.1}_{-1.1}$

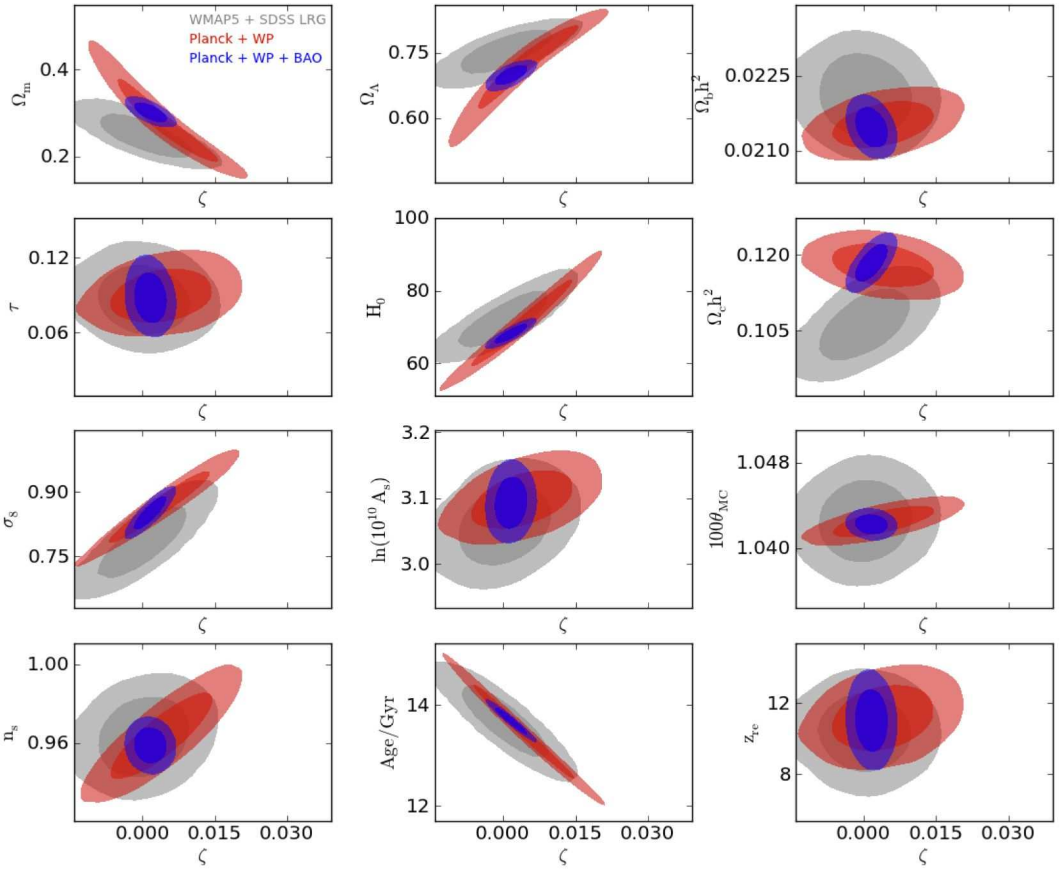

FIG. 5: The two dimensional contour for cosmological parameters.